Give Me FP32 or Give Me Death?
Challenges and Solutions for Reproducible Reasoning

Jiayi Yuan[1]*   **Hao Li**[2]*   **Xinheng Ding**[2]   **Wenya Xie**[2]   **Yu-Jhe Li**[3]
Wentian Zhao[3]   **Kun Wan**[3]   **Jing Shi**[3]   **Xia Hu**[1]   **Zirui Liu**[2]
[1]Rice University   [2]University of Minnesota Twin Cities   [3]Adobe Inc.
{jy101,xia.hu}@rice.edu
{li003703,ding0499,xie00470,zrliu}@umn.edu
{jhel,wezhao,kuwan,jingshi}@adobe.com

Abstract

Large Language Models (LLMs) are now integral across various domains and have demonstrated impressive performance. Progress, however, rests on the premise that benchmark scores are both accurate and reproducible. We demonstrate that the reproducibility of LLM performance is fragile: changing system configuration such as evaluation batch size, GPU count, and GPU version can introduce significant difference in the generated responses. This issue is especially pronounced in reasoning models, where minor rounding differences in early tokens can cascade into divergent chains of thought, ultimately affecting accuracy. For instance, under bfloat16 precision with greedy decoding, a reasoning model like DeepSeek-R1-Distill-Qwen-7B can exhibit up to **9% variation in accuracy and 9,000 tokens difference in response length due to differences in GPU count, type, and evaluation batch size.** We trace the root cause of this variability to the non-associative nature of floating-point arithmetic under limited numerical precision. This work presents the first systematic investigation into how numerical precision affects reproducibility in LLM inference. Through carefully controlled experiments across various hardware, software, and precision settings, we quantify when and how model outputs diverge. Our analysis reveals that floating-point precision—while critical for reproducibility—is often neglected in evaluation practices. Inspired by this, we develop a lightweight inference pipeline, dubbed *LayerCast*, that stores weights in 16-bit precision but performs all computations in FP32, balancing memory efficiency with numerical stability. Code is available at https://github.com/nanomaoli/llm_reproducibility.

1 Introduction

Large Language Models (LLMs) are increasingly being deployed in everyday scenarios, powering applications from chatbots [2] to automated coding tools [23] and personalized healthcare agents [6]. As their impact grows, rigorous benchmarking and evaluation become critical to measure real progress and ensure reliability, safety, and fairness [7, 34]. There are two commonly used evaluation strategies. The first one is to use *greedy decoding* by setting the temperature to zero, which produces deterministic outputs, and reports the result from a single run. The second uses *random sampling* with a non-zero temperature and reports performance using the Pass@K metric [8], i.e., the probability that at least one of K independent solution attempts will succeed.

In this paper, we highlight a commonly overlooked factor in both evaluation settings: **numerical precision**. First, for the greedy decoding setting, this factor undermines the assumption of determin-
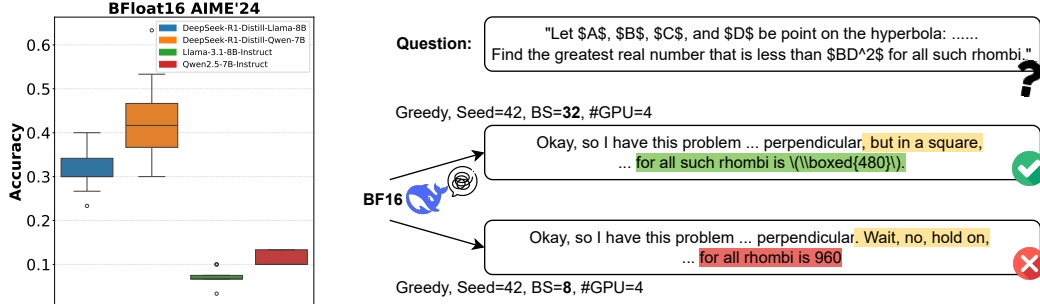
---
*Equal contribution

Figure 1: **Left:** Under BF16 precision and greedy decoding, the model's output can vary significantly depending on factors such as GPU count, evaluation batch size, and GPU hardware version. **Right:** For example, changes in evaluation batch size alone can lead to noticeable differences in responses, which is often ignored and not standardized by evaluation benchmarks.

ism–even with the same prompt and random seed, the generated output can still differ significantly between different hardware and system configurations. Second, for the random sampling setting, the numerical error demands a larger number of runs to control the variance. Surprisingly, we found that the results can be significantly different under the greedy decoding when changing the evaluation batch size, number of GPUs, or GPU versions. Through analysis, we found that the root cause of this problem is the non-associative property floating-point arithmetic, meaning $(a + b) + c \neq a + (b + c)$ due to finite precision and rounding errors. This issue is particularly problematic for recent reasoning-focused models [13], which generate very long chains of thought. In such cases, small numerical errors accumulate during the token generation process, eventually leading to significant differences in output across different runs. As illustrated in Figure 1, the model produces significantly different outputs when the number of GPUs, evaluation batch size, or hardware versions change—even if the same random seed and greedy decoding are used. This inconsistency makes it difficult to reproduce results, posing a serious problem for measuring the progress.

We highlight the significance of this issue for several critical reasons. First, many researchers report benchmark performance based on a single inference run with a fixed random seed to reduce computational cost. However, as shown in Figure 1. This practice can lead to misleading conclusions about model performance. Second, even when performing random sampling with multiple independent runs, the averaged results can still vary significantly due to hardware and system-level non-determinism. Moreover, when researchers report standard deviations without accounting for this numerical non-determinism, they risk severely overestimating a model's true uncertainty, since the reported variance reflects a mixture of intrinsic model uncertainty and variance introduced by finite numerical precision. When results cannot be exactly reproduced, it becomes difficult to distinguish whether improvements are from better methods or merely random variation.

To fill this gap, we conduct a comprehensive analysis of how numerical precision and hardware configurations affect the reproducibility of LLMs. **Our findings show that inference using the commonly adopted BF16 precision is highly sensitive to variations in hardware and system configurations, such as tensor parallel size, evaluation batch size, and GPU types.** These hardware-related factors are often beyond users' control and can vary significantly due to resource availability, yet they are often overlooked in current LLM evaluation methods. We observe that increasing the number of mantissa bits in the numerical format—such as using FP16 or FP32—can significantly mitigate this issue. Based on these findings, we propose an optimized inference pipeline that performs all computations in FP32 while retaining model weights in BF16 precision. This approach effectively balances memory efficiency and reproducibility. Specifically, our contributions and suggestions can be summarized as follows:

- **Extensive analysis of how numerical precision affects reproducibility in both greedy decoding and random sampling scenarios.** Our finding suggests that due to the limited precision, the model performance is highly sensitive to variations in hardware and system configurations, such as tensor parallel size, evaluation batch size, and GPU types.

- **Practical suggestions for reproducible reasoning to the community**. Based on our findings, we suggest (1) If sufficient computational resources are available, please use random sampling (non-zero temperature) with multiple runs. Report the mean accuracy, average answer length, and
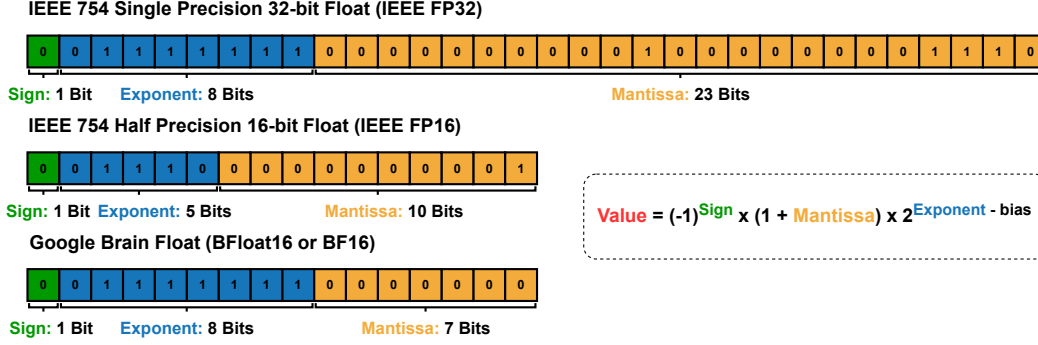
Figure 2: Floating-point format of FP32, FP16 and BF16.

error bars. Note that with 16-bit precision and small datasets, more trials are needed for stable results in general. (2) If using greedy decoding with a single run, please use FP32 precision to improve the reproducibility of your results.

- **An optimized FP32 inference pipeline**. We propose an optimized inference pipeline called LayerCast, which performs all computations in FP32 while retaining model weights in BF16 precision. This approach effectively balances memory efficiency and reproducibility. We release it as a patch to vLLM and and can be used with just a few lines of code change.

2 Preliminary

2.1 Current Practices on LLM Reproducibility

There are two widely adopted evaluation strategies. The first one is *greedy decoding*, where temperature is set to zero and model always select the token with highest probability. The second strategy employs *random sampling* with a non-zero temperature, and evaluates performance using the Pass@K metric [8]. Below we introduce the commonly adopted experimental setting for the reproducibility.

Greedy decoding is a deterministic text generation strategy where the model always selects the token with the highest probability at each step. In theory, this approach should produce identical outputs given the same input and model parameters. However, in this paper, we show that even greedy decoding can yield different results across runs due to numerical precision issues.

Random sampling selects output tokens based on the model's probability distribution with a non-zero temperature to introduce randomness. The most commonly used evaluation metric is the mean accuracy across multiple independent trials, which is equivalent to Pass@1 [8].

Deterministic libraries and Random Seeds. Random seeds in LLM generation control the pseudo-random number generator that selects tokens when using non-greedy decoding. It is a standard practice to fix random seeds; however, this is not always sufficient for ensuring full determinism in greedy decoding. Even with a fixed seed, differences in computation order can alter the sequence of the pseudo-random number generator [15]. Meanwhile, frameworks like PyTorch and TensorFlow provide flags for deterministic behavior (e.g., `torch.use_deterministic_algorithms(True)` [2]). These ensure that certain operations avoid algorithms that could produce different results across runs. However, in practice, it can still produce non-deterministic results even with these flags .

Despite these efforts, achieving perfect reproducibility in LLM inference remains a challenge. The next subsection delves into a crucial factor that often leads to non-deterministic behavior even with greedy decoding and the aforementioned practices in place.

2.2 Numerical Precision and Rounding Errors

Numerical precision is critical for reproducibility [24]. Higher precision numbers have less rounding error, which can reduce variability in results. Examples include using FP32 for certain parts of computation—like softmax or attention scores—even if the model weights are in 16-bit precision.

---

[2] https://pytorch.org/docs/stable/generated/torch.use_deterministic_algorithms.html

Table 2: Two illustrative cases demonstrate how rounding error arising from the non-associativity of floating-point addition can affect numerical results. Example 1 reveals accumulation error at both precisions; Example 2 exhibits a discrepancy only in BF16, while FP32 delivers identical results, illustrating higher-precision numeric types are more tolerant of rounding errors.

Example	Sum Order	FP32	BF16
$a, b, c = 0.1, -0.1, 0.2$	$a + b + c$	00111110010011001100110011001101	0011111001001101
	$a + c + b$	00111110010011001100110011001110	0011111001001110
$a, b, c = 0.0016, 0.0027, 1.0$	$a + b + c$	00111111100000001000110011100111	0011111110000001
	$a + c + b$	00111111100000001000110011100111	0011111110000000

This practice can mitigate run-to-run differences, but it doesn't provide theoretical guarantees since floating-point arithmetic cannot represent all real numbers exactly. Even with the same precision, different hardware implementations or computation orders can lead to slightly different results. In this paper, we primarily focus on the importance of numerical precision and provide a detailed analysis of its impact on LLM inference reproducibility.

Table 1: Rounding error when the same true value (1.00012) is represented in three different numeric formats.

Precision	Decimal	Rounding Error
FP32	1.00012004375457761	$\approx +4.38\mathrm{e}{-8}$
FP16	1.0	≈ -0.00012
BF16	1.0	≈ -0.00012

Figure 2 shows the format of BF16, FP16 and FP32. Table 1 illustrates the rounding error that occurs when the same true value is represented in three different numeric formats. As expected, lower precision formats like FP16 and BF16 introduce larger rounding errors compared to FP32.

Moreover, a key aspect of floating-point arithmetic that contributes to non-determinism is its non-associativity. This means that the order in which numbers are added can affect the final result due to accumulated rounding errors. Table 2 provides illustrative examples of how the order of summation can lead to different results in FP32 and BF16. This becomes particularly relevant in the parallel computations performed in GPUs during LLM inference.

In the context of LLMs, even small numerical variations in the logit values can affect the final token selection when the top probabilities are close. Floating-point arithmetic in GPUs exhibits non-associativity, meaning $(a + b) + c \neq a + (b + c)$ due to finite precision and rounding errors. This property directly impacts the computation of attention scores and logits in the transformer architecture, where parallel operations across multiple threads can yield different results based on execution order. Formally, for a reduction operation $\oplus$ over a set of values $\{v_1, v_2, ..., v_n\}$ (such as summing attention scores or computing softmax denominators), the result depends on the specific ordering of operations:

$$\bigoplus_{i=1}^{n} v_i = v_{\pi(1)} \oplus v_{\pi(2)} \oplus ... \oplus v_{\pi(n)},$$

where π is a permutation of indices $\{1, 2, ..., n\}$ determined by thread scheduling.

3 Reproducibility Issues with Limited Numerical Precision

3.1 Experiment Setup

We conduct experiments on four recent LLMs, including two reasoning models: DeepSeek-R1-Distill-Qwen-7B, DeepSeek-R1-Distill-Llama-8B and two non-reasoning models: Qwen2.5-7B-Instruct and Llama-3.1-8B-Instruct [13, 32, 21], across five commonly used LLM evaluation benchmarks: AIME'24, MATH500, LiveCodeBench-Easy, LiveCodeBench-Medium, and LiveCodeBench-Hard [1, 14, 17]. For reasoning models, we set the maximum output token length to 32,768 and for non-reasoning models, we set it to 2,048. We use vLLM [19] as the inference backend. In the random sampling experiments, we set *temperature* to 0.7 and *top-p* to 0.95. Our Evaluation implementation and prompt setting is adapted from SkyThought-evals [27], more details can be found in Appendix C.

For each model-task pair, we evaluate under 12 different runtime configurations, representing all combinations of 2 GPU types (NVIDIA L40S and A100), 2 GPU counts (2 and 4), and 3 batch sizes (8, 16, and 32), i.e., $2 \times 2 \times 3 = 12$ different configurations, to simulate the diversity of deployment environments encountered in real-world evaluations. Unlike decoding parameters or random seeds, these hardware-related factors are often beyond users' control and can vary significantly due to resource availability, yet they are often overlooked in current LLM evaluation methods.

To comprehensively quantify output instability and better analyze the impact of numerical precision on inference variability, we evaluate the reproducibility under both greedy decoding and random sampling settings. Specifically, for greedy decoding, we analyze:

- **Std@Acc** (Standard deviation of accuracy): For each numerical precision, we evaluate accuracy under the 12 different runtime configurations and compute their sample standard deviations, which serve as indicators of the stability of LLM inference outputs during greedy inference.
- **Avg_Std@Output_Length** (Average standard deviation of output length): We measure the length of output tokens, compute the sample standard deviation per example across 12 runtime configurations, and report the mean of standard deviations over the entire dataset. This provides an alternative perspective on the stability of LLM inference outputs during greedy inference.
- **Div_Index** (Divergence index): For the same question, ixf two or more responses produce identical token sequences up to a certain position, but generate different tokens after that position, we define the index of that position as the divergence index. A higher **Div_Index** indicates greater consistency across responses under different runtime configurations.
- **Avg_Std@top1_prob** (Average standard deviation of top-1 token prediction probability): Before divergence, all responses across different runtime settings produce identical top-1 tokens at every position. However, due to floating-point computation errors, the predicted probabilities of these tokens may vary across settings. To quantify this, we compute the standard deviation of the predicted probability for the top-1 token at each position across settings, then average over all positions from 0 to Div_Index and over all examples in a dataset. We define this metric as the Average Standard Deviation of Top-1 Token Prediction Probability, which serves as an indicator of the magnitude of numerical variation introduced by floating-point errors.

For random sampling, we analyze:

- **Pass@1**: For each numerical precision, we evaluate performance by running the model multiple times and computing the average accuracy accuracy (commonly referred to as Pass@1). Specifically, we use both 16 and 64 independent runs to compute mean accuracy for AIME'24, and 4 independent runs for MATH500. To assess the stability of random sampling-based decoding, we also report the standard deviation of Pass@1 across 6 runtime configurations, varying GPU count (2 vs. 4) and numerical precision (BF16, FP16, FP32).

3.2 Greedy Decoding $\neq$ Deterministic Output

Contrary to common belief, our experiments reveal that greedy decoding does not guarantee deterministic outputs across different hardware and system configurations. However, using FP32 precision helps a lot. Table 3 presents the standard deviation of accuracy (Std@Acc) across 12 runtime configurations for BF16, FP16 and FP32 precisions. The results demonstrate a clear pattern: FP32 consistently achieves near-perfect reproducibility with negligible variance, FP16 shows moderate variability, while BF16 exhibits substantial instability. This pattern is particularly pronounced for reasoning models like DeepSeek-R1-Distill-Qwen-7B, where BF16 precision introduces up to 9% standard deviation in accuracy on AIME'24, compared to virtually zero variance under FP32. This

Table 3: Std@Acc of greedy decoding across 12 different settings (GPU types, GPU counts, and batch sizes) under BF16, FP16, and FP32 Numerical Precisions. Reasoning models also exhibit larger variance compared to non-reasoning counterparts. More results can be found in Appendix E.

	AIME'24			MATH500			LiveCodeBench-Easy		
	BF16	**FP16**	**FP32**	**BF16**	**FP16**	**FP32**	**BF16**	**FP16**	**FP32**
DeepSeek-R1-Distill-Qwen-7B	9.15%	5.74%	0	1.04%	1.12%	0.12%	1.67%	1.28%	0.37%
DeepSeek-R1-Distill-Llama-8B	4.60%	6.00%	5.8e-17	1.59%	0.73%	0.23%	2.31%	1.92%	0.29%
Qwen2.5-7B-Instruct	1.71%	1.45e-17	1.45e-17	0.83%	0.36%	1.16e-16	0.79%	0.48%	1.16e-16
Llama-3.1-8B-Instruct	1.92%	1.30%	0	0.94%	0.34%	0.13%	1.00%	0.67%	0.25%

Table 4: Standard deviation of output length of greedy decoding across 12 different settings (GPU types, GPU counts, and batch sizes) under BF16, FP16, and FP32 numerical precisions. The output length of reasoning models exhibit large variance. More results can be found in Appendix E.

	AIME'24			MATH500			LiveCodeBench-Easy		
	BF16	**FP16**	**FP32**	**BF16**	**FP16**	**FP32**	**BF16**	**FP16**	**FP32**
DeepSeek-R1-Distill-Qwen-7B	9189.53	5990.32	0	2774.28	2090.46	138.75	5507.52	4282.78	262.55
DeepSeek-R1-Distill-Llama-8B	9348.59	7822.43	0	4015.00	2518.38	146.03	4732.85	3652.16	105.85
Qwen2.5-7B-Instruct	211.47	48.14	0	52.61	15.37	0	7.79	0.71	0
Llama-3.1-8B-Instruct	119.21	49.73	0	124.43	40.57	2.76	31.03	4.70	0.49

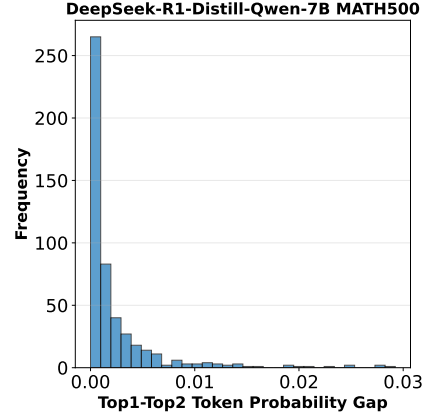| Answer 1		Answer 2	
Token	Prob.	Token	Prob.
know	49.75%	have	46.65%
have	43.91%	know	46.64%
need	3.18%	need	3.39%
'm	2.47%	'm	2.63%
've	0.49%	've	0.52%
...	...	...	...

Figure 3: **Left:** the top-5 tokens and their predicted probabilities at the divergence index for two different answers to the same question in BF16. **Right:** The gap between the top-two competing tokens probability. We observe the token probability gap are often minimal in reasoning models.

finding is concerning because it suggests that **using different GPU types or varying the number of GPUs can *prevent you from reproducing* others' results, even when using greedy decoding.** Beyond accuracy variance, our results in Table 4 reveal that **BF16 precision also causes response lengths to vary significantly across different settings.** This raises significant concerns for recent work in efficient reasoning and long-to-short research [25], which needs to report response length metrics. Specifically, changing the system configuration can lead to a difference of up to 9,000 tokens in response length. This variability undermines the effectiveness of many existing efficient reasoning approaches. However, our findings show that using FP16 helps reduce output length variance to some extent, while FP32 offers the most consistent and reliable control over this variability. **Thus, we suggest if using greedy decoding, please use FP32 precision to improve the reproducibility of the efficient reasoning research.**

The performance gap clearly indicates that across different runs, the model generates different tokens. To investigate why this happens, we compared outputs from different runs. Since we are using greedy decoding, the top-1 probability token differs between runs at the point of divergence. Figure 3 shows an example of token logits when two runs diverge, illustrating how numerical precision errors can flip the order of the top-1 and top-2 token probabilities. Figure 3 also shows the histogram of probability differences between top-1 and top-2 tokens under FP32 precision. We observe that **for reasoning models, the token probability differences between the top two competing tokens are often minimal**.

To further understand how this observation interacts with the numerical errors, Figure 4 further illustrates the average standard deviation of the probability of prediction of the top-1 token (Avg_Std@Top1_Prob) at different numerical precision levels. BF16 shows significantly higher variance in top-1 token probabilities compared to FP16 and FP32. This increased variance arises because BF16's limited mantissa bits (7 bits compared to FP16's 10 bits) introduce larger errors in probability computations, increasing the likelihood of token flips when these fluctuations overlap with the small gap between top-1 and top-2 candidate tokens. In contrast, FP32's higher precision (23 mantissa bits) makes runtime variations nearly negligible. Together, these results demonstrate that
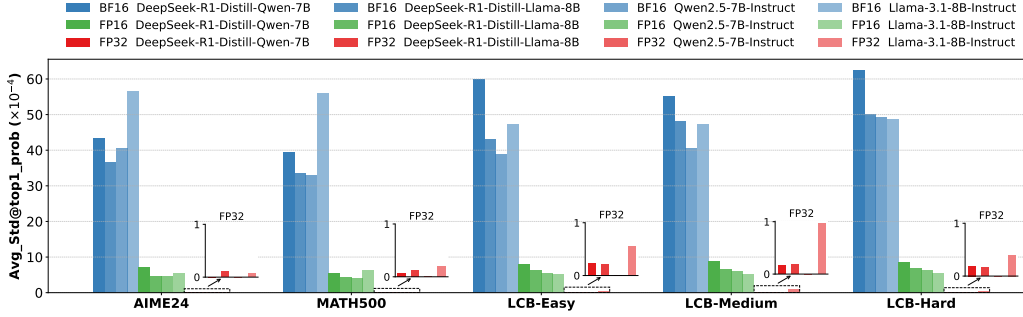
Figure 4: Avg_Std@top1_prob across 12 different settings for 4 models and 5 tasks, under BF16, FP16 and FP32. FP16 shows significantly lower variance compared to BF16. FP32 yields near-zero variance, demonstrating strong robustness to floating-point rounding errors.

token selection during greedy decoding is highly sensitive to even small numerical variations because of the minimal probability differences between competing tokens.

The impact of numerical precision on output stability is further evidenced by divergence patterns in greedy decoding. Figure 5 shows the distribution of divergence points (Div_Index) across precision formats for DeepSeek-R1-Distill-Qwen-7B on MATH500. As precision increases from BF16 to FP32, we observe both fewer divergent examples overall and a significant shift in when divergence occurs. With FP32, almost all examples produce identical outputs across configurations, resulting in only 2.2% of the samples diverged. In contrast, with BF16, divergence frequently occurs early in generation despite the deterministic setting, with over 90% of examples showing some form of divergence. When divergence happens in higher precision formats, it typically occurs much later in the sequence, limiting its impact on the final output and answer accuracy.
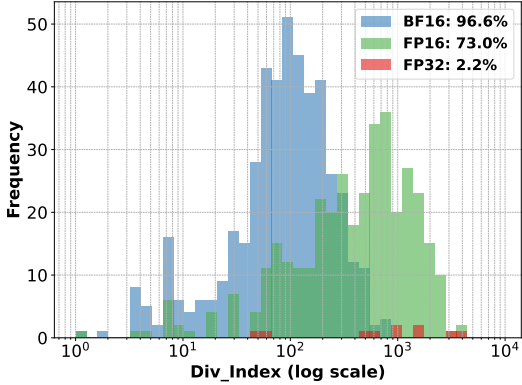

Figure 5: Distribution of Div_Index for DeepSeek-R1-Distill-Qwen-7B on MATH500 under BF16, FP16, and FP32. Higher numerical precision leads to much fewer divergent examples and a shift of divergence onset to later token positions.

These results conclusively demonstrate that numerical precision is a critical factor in achieving truly deterministic outputs with greedy decoding, with higher precision formats providing substantially better reproducibility.

3.3 Random Sampling Has Reproducibility Issue, Too

One might argue that while greedy decoding is vulnerable to token-level instability from numerical precision, random sampling might be less sensitive due to its intrinsic stochasticity. **However, our experiments reveal that numerical precision significantly affects the stability and reproducibility of sampling-based evaluations as well.** When using random sampling with temperature $T > 0$, researchers typically report the mean accuracy averaged over multiple runs (commonly referred to as Pass@1). We conduct Pass@1 evaluations across two benchmarks–AIME'24 and MATH500–using 16 and 64 independent sampling runs for AIME'24 and 4 runs for MATH500. Here we emphasize that in Table 5, the reported standard deviation is calculated based on Pass@1 performance across 6 system configurations per model (batch sizes and GPU counts), not across repeated runs of the same configuration. Thus, the reported variance largely reflects the impact from limited numerical precision, not the inherent variance of models. As shown in Table 5, we observe a clear trend: numerical precision introduces an additional source of variance beyond the intended randomness, and lower-precision formats such as BF16 tend to produce higher output variance. See Appendix H for the complete Pass@1 results that support these variance statistics.

Table 5: Standard deviation of Pass@1 performance (%) under different GPU counts and precisions. We emphasize that the reported values reflect **the variability of Pass@1 performance across 6 different system configurations** (3 batch sizes × 2 GPU counts), *not* across repeated runs of the same configuration.

	MATH500 (n=4)			AIME'24 (n=16)			AIME'24 (n=64)		
	BF16	**FP16**	**FP32**	**BF16**	**FP16**	**FP32**	**BF16**	**FP16**	**FP32**
DeepSeek-R1-Distill-Qwen-7B	0.3158	0.1463	0.1021	1.7151	0.8273	1.1785	0.3749	0.5391	0.7377
DeepSeek-R1-Distill-Llama-8B	0.3602	0.3371	0.1211	1.5124	1.8792	0.8606	0.8774	0.8539	0.5034
Qwen2.5-7B-Instruct	0.4663	0.1686	0.0274	0.7056	0.2523	0	0.1784	0.1382	0
Llama-3.1-8B-Instruct	0.6020	0.1725	0.3293	0.5992	0.2282	0.7759	0.4216	0.2898	0.1296

This pattern largely holds across the models we evaluate, especially on the MATH500 benchmark. A notable exception arises in the AIME'24 results for DeepSeek-R1-Distill-Qwen-7B, where at n = 64, FP32 exhibits higher variance (0.7377) than BF16 (0.3749). We interpret this as a result of dataset size and sampling dynamics rather than a contradiction of the overall trend. With only 30 problems in AIME'24, a single answer can shift Pass@1 by about 3.33%, amplifying statistical noise. Moreover, BF16–which exhibits the highest variance at n = 16–also shows the greatest improvement when increasing to n = 64. This suggests that instability from reduced numerical precision can be mitigated with sufficient averaging, but remains a dominant factor at typical sample sizes.

These findings highlight numerical precision as a critical factor in the reproducibility of sampling-based evaluations. Researchers using random sampling with BF16 may need substantially more runs to achieve the same statistical confidence as with higher-precision formats, representing a computational overhead that is rarely acknowledged in current evaluation practices.

3.4 Ablation: How Runtime Configurations Affect Reproducibility

After establishing that numerical precision plays a crucial role in LLM reproducibility, we now investigate how specific runtime configurations—batch size, number of GPUs, and GPU type—affect output stability across different precision formats. We conduct experiments of *greedy decoding* setting on DeepSeek-R1-Distill-Qwen-7B, as shown in Figure 6.

Our analysis of runtime configurations reveals three key factors affecting token probability variations. First, in Figure 6 (a), configurations with 4 GPUs tend to exhibit higher probability variation than those with 2 GPUs across 3 tested batch sizes (particularly in BF16 precision), potentially due to increased parallel computation introducing more varied floating-point operation orderings and consequently different rounding errors. Second, Figure 6 (b) suggests that smaller batch sizes counter-intuitively produce higher variance in token probabilities because they may require more sequential processing steps that accumulate rounding errors, while larger batches benefit from
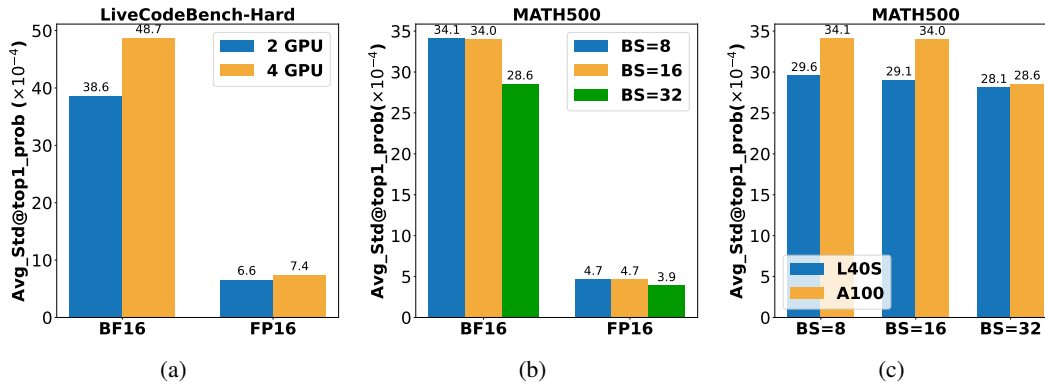

Figure 6: Controlled experiments for Avg_Std@top1_prob under different runtime configurations: (a) **2GPU vs 4GPU** (varying batch size); (b) **BS=8 vs 16 vs 32** (varying A100 GPU Count); (c) **L40S vs A100** (BF16, varying GPU Count). Larger GPU counts and smaller batch sizes tend to increase inference instability.
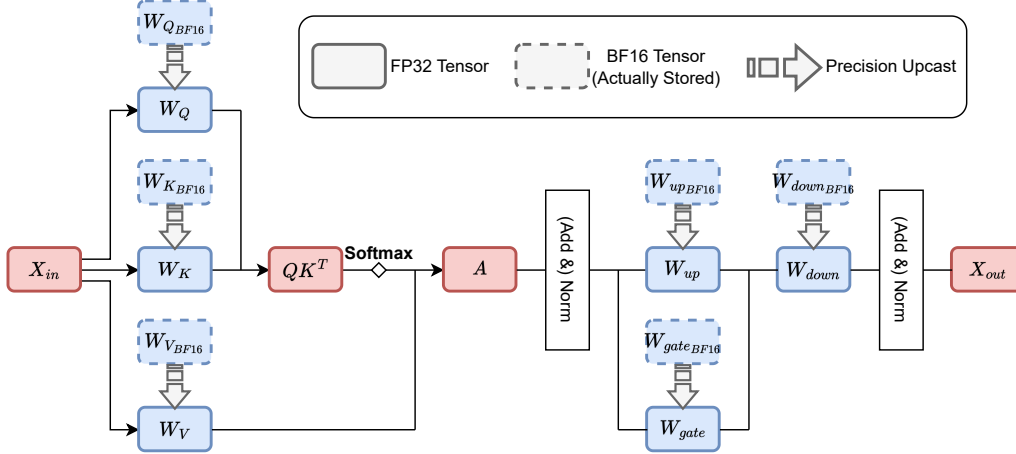
Figure 7: Workflow of LayerCast within one transformer block. Here we omit skip connections, position embeddings and activation functions.

parallel computation within optimized CUDA kernels that limit error accumulation. Third, GPU architecture matters: Figure 6 (c) shows A100s generally exhibit slightly higher probability variance than L40S under identical configurations, likely due to differences in hardware-level floating-point implementations and memory hierarchies. All these effects are most pronounced under BF16 precision with its limited mantissa bits making it especially susceptible to rounding effects. For more results of runtime configurations and tested tasks, please refer to the Appendix F.

In summary, our experiments reveal three critical insights about numerical precision and reproducibility in LLM inference. **First**, the fundamental cause of nondeterministic outputs is the small gap between competing logits, which makes token selection vulnerable to minute numerical fluctuations. **Second**, precision format critically impacts stability, with FP32 providing near-perfect determinism, FP16 offering moderate stability, and BF16 exhibiting significant variance despite being commonly used. **Third**, specific runtime configurations—particularly GPU count, batch size, and GPU architecture—further affect reproducibility, with these effects most pronounced in lower precision formats. These findings highlight the urgent need for standardized evaluation practices that account for numerical precision effects, especially as LLMs continue to be deployed in increasingly critical applications where reproducibility is essential.

4 Near-Perfect Deterministic Reproduction: LayerCast

Given our findings on when and why reproducibility breaks, we now propose directions to improve reproducibility in LLM inference. The basic solution is using FP32 precision, as we've shown in previous sections. However, this approach incurs significant costs: it doubles the memory usage and inference time compared to BF16, making it impractical for many production environments.

We propose a more efficient solution: LayerCast, a hybrid precision approach that balances computational stability with memory efficiency. LayerCast works by: (1) Loading the model parameters initially in FP32 precision; (2) Explicitly casting all linear layer weights and biases to BF16 for storage before inference; and (3) As inference runs, upcasting each weight back to FP32 just-in-time for matrix multiplication, **one at a time.**

Figure 8: Distribution of Div_Index for DeepSeek-R1-Distill-Qwen-7B on MATH500 under BF16, FP32, and LayerCast.

As illustrated in Figure 7, this approach ensures all computations occur in full FP32 precision while storing weights in memory-efficient 16-bit formats. Thus, this model benefits from FP32's stability
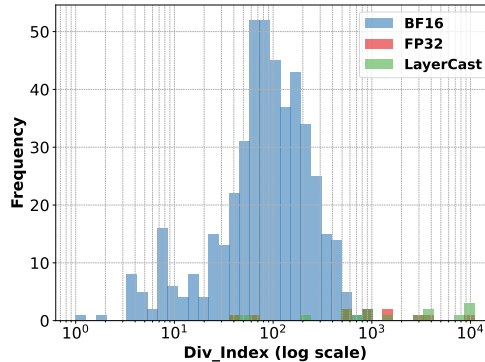
9

during computation, while the memory footprint remains closer to that of 16-bit models. This provides determinism comparable to full FP32 inference but with substantially reduced memory requirements, particularly beneficial for the KV cache in long-context scenarios.

Our experimental results strongly support this approach. When examining the standard deviation of accuracy across runs, Layer Cast achieves stability nearly identical to FP32, while BF16 shows much higher variability. As shown in Figure 8, the divergence index measurements further confirm that LayerCast produces consistent outputs across different batch sizes and GPU configurations, with divergence rates below 3.4%. From resource perspective, LayerCast offers substantial benefits over full FP32: memory usage is reduced by 34% (particularly important for KV cache in long-context scenarios). These improvements make LayerCast a practical solution for applications requiring both deterministic outputs and reasonable performance. For full result, please refer to Appendix G.

5 Related Works

Since the era of traditional deep learning, the reproducibility of models [26, 36, 31] have remained complex and challenging problems that have yet to be fully resolved. As large language models (LLMs) have risen to prominence, numerous empirical studies [20, 33, 3, 11, 18, 30, 22, 35] have shown that nondeterministic behavior during LLM inference is widely observed. Existing study [5] have found a clear negative correlation between output length and inference consistency: As the length of generated text increases, output variation during inference also rises, which explains the phenomenon that reasoning models tend to exhibit greater inference uncertainty.

Multiple factors can affect the reproducibility of LLM inference results, including but not limited to prompt formatting, decoding parameters (such as temperature and top-p thresholds), random seed settings, and hardware and software configurations [16, 10, 9]. Existing studies [22, 11, 3, 20, 4] have systematically analyzed the impact of decoding parameters (e.g., temperature, top-p) on the stability of LLM inference outputs. Hochlehnert et al. [15] points out that many reported improvements in LLM performance are, in fact, partially attributable to unfair comparisons and unreported sources of variance in the evaluation process. In practical applications, using FP32 (single-precision floating point) inference [28, 29] is often empirically believed to enhance the robustness of numerical computations. Feng et al. [12] investigates the impact of numerical precision on the mathematical reasoning ability of LLMs. However, there is currently a lack of systematic and quantitative studies specifically analyzing the effects of different numerical formats (e.g., FP32, FP16, BF16) on the reproducibility of LLM inference.

6 Conclusion

In this paper, we conducted a comprehensive investigation into the reproducibility challenges in LLM inference caused by numerical precision issues. Our experiments across multiple models, tasks, and hardware configurations revealed that even under supposedly deterministic greedy decoding, outputs can vary significantly due to floating-point arithmetic non-associativity. We demonstrated that precision format critically impacts stability, with FP32 providing near-perfect determinism while BF16—despite being widely used—exhibits substantial variance. To address these challenges without incurring the full overhead of FP32, we proposed LayerCast, a practical solution that achieves FP32-level determinism while maintaining reasonable memory efficiency. Our findings highlight the importance of standardizing evaluation practices to account for numerical precision effects, especially as LLMs are increasingly deployed in critical applications where reproducibility is essential.

References

[1] Aime 2024 dataset. `https://huggingface.co/datasets/Maxwell-Jia/AIME_2024`.

[2] Josh Achiam, Steven Adler, Sandhini Agarwal, Lama Ahmad, Ilge Akkaya, Florencia Leoni Aleman, Diogo Almeida, Janko Altenschmidt, Sam Altman, Shyamal Anadkat, et al. Gpt-4 technical report. *arXiv preprint arXiv:2303.08774*, 2023.

[3] Chetan Arora, Ahnaf Ibn Sayeed, Sherlock Licorish, Fanyu Wang, and Christoph Treude. Optimizing large language model hyperparameters for code generation. *arXiv preprint arXiv:2408.10577*, 2024.

[4] Berk Atil, Sarp Aykent, Alexa Chittams, Lisheng Fu, Rebecca J. Passonneau, Evan Radcliffe, Guru Rajan Rajagopal, Adam Sloan, Tomasz Tudrej, Ferhan Ture, Zhe Wu, Lixinyu Xu, and Breck Baldwin. Non-determinism of "deterministic" llm settings, 2025.

[5] Berk Atil, Alexa Chittams, Liseng Fu, Ferhan Ture, Lixinyu Xu, and Breck Baldwin. Llm stability: A detailed analysis with some surprises. *arXiv preprint arXiv:2408.04667*, 2024.

[6] Marco Cascella, Jonathan Montomoli, Valentina Bellini, and Elena Bignami. Evaluating the feasibility of chatgpt in healthcare: an analysis of multiple clinical and research scenarios. *Journal of medical systems*, 47(1):33, 2023.

[7] Yupeng Chang, Xu Wang, Jindong Wang, Yuan Wu, Linyi Yang, Kaijie Zhu, Hao Chen, Xiaoyuan Yi, Cunxiang Wang, Yidong Wang, et al. A survey on evaluation of large language models. *ACM transactions on intelligent systems and technology*, 15(3):1–45, 2024.

[8] Mark Chen, Jerry Tworek, Heewoo Jun, Qiming Yuan, Henrique Ponde De Oliveira Pinto, Jared Kaplan, Harri Edwards, Yuri Burda, Nicholas Joseph, Greg Brockman, et al. Evaluating large language models trained on code. *arXiv preprint arXiv:2107.03374*, 2021.

[9] Huggingface Docs. Reproducibility. `https://huggingface.co/docs/diffusers/v0.14.0/en/using-diffusers/reproducibility`, 2025. Accessed: 2025-04-28.

[10] PyTorch Docs. Reproducibility. `https://pytorch.org/docs/stable/notes/randomness.html`, 2025. Accessed: 2025-04-28.

[11] Benedetta Donato, Leonardo Mariani, Daniela Micucci, and Oliviero Riganelli. Studying how configurations impact code generation in llms: the case of chatgpt. *arXiv preprint arXiv:2502.17450*, 2025.

[12] Guhao Feng, Kai Yang, Yuntian Gu, Xinyue Ai, Shengjie Luo, Jiacheng Sun, Di He, Zhenguo Li, and Liwei Wang. How numerical precision affects mathematical reasoning capabilities of llms. *arXiv preprint arXiv:2410.13857*, 2024.

[13] Daya Guo, Dejian Yang, Haowei Zhang, Junxiao Song, Ruoyu Zhang, Runxin Xu, Qihao Zhu, Shirong Ma, Peiyi Wang, Xiao Bi, et al. Deepseek-r1: Incentivizing reasoning capability in llms via reinforcement learning. *arXiv preprint arXiv:2501.12948*, 2025.

[14] Dan Hendrycks, Collin Burns, Saurav Kadavath, Akul Arora, Steven Basart, Eric Tang, Dawn Song, and Jacob Steinhardt. Measuring mathematical problem solving with the math dataset. *arXiv preprint arXiv:2103.03874*, 2021.

[15] Andreas Hochlehnert, Hardik Bhatnagar, Vishaal Udandarao, Samuel Albanie, Ameya Prabhu, and Matthias Bethge. A sober look at progress in language model reasoning: Pitfalls and paths to reproducibility. *arXiv preprint arXiv:2504.07086*, 2025.

[16] Ingonyama. Solving reproducibility challenges in deep learning and llms: Our journey. `https://www.ingonyama.com/post/solving-reproducibility-challenges-in-deep-learning-and-llms-our-journey`, 2025. Accessed: 2025-04-28.

[17] Naman Jain, King Han, Alex Gu, Wen-Ding Li, Fanjia Yan, Tianjun Zhang, Sida Wang, Armando Solar-Lezama, Koushik Sen, and Ion Stoica. Livecodebench: Holistic and contamination free evaluation of large language models for code. *arXiv preprint arXiv:2403.07974*, 2024.

[18] Eugene Klishevich, Yegor Denisov-Blanch, Simon Obstbaum, Igor Ciobanu, and Michal Kosinski. Measuring determinism in large language models for software code review. *arXiv preprint arXiv:2502.20747*, 2025.

[19] Woosuk Kwon, Zhuohan Li, Siyuan Zhuang, Ying Sheng, Lianmin Zheng, Cody Hao Yu, Joseph Gonzalez, Hao Zhang, and Ion Stoica. Efficient memory management for large language model serving with pagedattention. In *Proceedings of the 29th Symposium on Operating Systems Principles*, pages 611–626, 2023.

[20] Jiawei Liu, Chunqiu Steven Xia, Yuyao Wang, and Lingming Zhang. Is your code generated by chatgpt really correct? rigorous evaluation of large language models for code generation. *Advances in Neural Information Processing Systems*, 36:21558–21572, 2023.

[21] Meta. Introducing llama 3.1: Our most capable models to date. `https://ai.meta.com/blog/meta-llama-3-1/`, 2024. Accessed: 2025-05-13.

[22] Shuyin Ouyang, Jie M Zhang, Mark Harman, and Meng Wang. An empirical study of the non-determinism of chatgpt in code generation. *ACM Transactions on Software Engineering and Methodology*, 34(2):1–28, 2025.

[23] Baptiste Roziere, Jonas Gehring, Fabian Gloeckle, Sten Sootla, Itai Gat, Xiaoqing Ellen Tan, Yossi Adi, Jingyu Liu, Romain Sauvestre, Tal Remez, et al. Code llama: Open foundation models for code. *arXiv preprint arXiv:2308.12950*, 2023.

[24] Sanjif Shanmugavelu, Mathieu Taillefumier, Christopher Culver, Oscar Hernandez, Mark Coletti, and Ada Sedova. Impacts of floating-point non-associativity on reproducibility for hpc and deep learning applications, 2024.

[25] Yang Sui, Yu-Neng Chuang, Guanchu Wang, Jiamu Zhang, Tianyi Zhang, Jiayi Yuan, Hongyi Liu, Andrew Wen, Shaochen Zhong, Hanjie Chen, and Xia Hu. Stop overthinking: A survey on efficient reasoning for large language models. *arXiv preprint arXiv:2503.16419*, 2025.

[26] Cecilia Summers and Michael J Dinneen. Nondeterminism and instability in neural network optimization. In *International Conference on Machine Learning*, pages 9913–9922. PMLR, 2021.

[27] NovaSky Team. Sky-t1: Train your own o1 preview model within $450. `https://novasky-ai.github.io/posts/sky-t1`, 2025. Accessed: 2025-01-09.

[28] vllm Issue 12343. Why are the vllm and hugging face transformers inference results inconsistent? `https://github.com/vllm-project/vllm/issues/12343`, 2025. Accessed: 2025-04-28.

[29] vllm Issue 12699. Different logprobs for qwn2-vl when running on transformers and on vllm. `https://github.com/vllm-project/vllm/issues/12699`, 2025. Accessed: 2025-04-28.

[30] Julian Junyan Wang and Victor Xiaoqi Wang. Assessing consistency and reproducibility in the outputs of large language models: Evidence across diverse finance and accounting tasks. *arXiv preprint arXiv:2503.16974*, 2025.

[31] Xiangzhe Xu, Hongyu Liu, Guanhong Tao, Zhou Xuan, and Xiangyu Zhang. Checkpointing and deterministic training for deep learning. In *Proceedings of the 1st International Conference on AI Engineering: Software Engineering for AI*, pages 65–76, 2022.

[32] An Yang, Baosong Yang, Beichen Zhang, Binyuan Hui, Bo Zheng, Bowen Yu, Chengyuan Li, Dayiheng Liu, Fei Huang, Haoran Wei, et al. Qwen2. 5 technical report. *arXiv preprint arXiv:2412.15115*, 2024.

[33] Boyang Yu. Benchmarking large language model volatility. *arXiv preprint arXiv:2311.15180*, 2023.

[34] Jiayi Yuan, Jiamu Zhang, Andrew Wen, and Xia Hu. The science of evaluating foundation models. *arXiv preprint arXiv:2502.09670*, 2025.

[35] Qiuhai Zeng, Claire Jin, Xinyue Wang, Yuhan Zheng, and Qunhua Li. An analyst-inspector framework for evaluating reproducibility of llms in data science. *arXiv preprint arXiv:2502.16395*, 2025.

[36] Donglin Zhuang, Xingyao Zhang, Shuaiwen Song, and Sara Hooker. Randomness in neural network training: Characterizing the impact of tooling. *Proceedings of Machine Learning and Systems*, 4:316–336, 2022.

A Limitations

Despite the importance of our work in highlighting and addressing numerical precision's effect on reproducibility, there are limitations that are worth noting. First, our experiments focus on a certain set of models and settings. Due to resource constraints, we do not conduct large-scale experiments on much larger models (>70B) or a wide range of GPU architectures or accelerators; these settings might exhibit different levels of numerical behaviors. Additionally, our study primarily addresses numerical precision issues in transformer-based LLMs and may not fully generalize to other architectures or modalities.

B Broader Impacts

This research has several societal impacts. First, by raising the discussion of reproducibility issues in LLM inference, our work promotes greater scientific rigor in AI research, calling for a more reliable comparison of models and techniques. This is particularly important as LLMs are increasingly deployed in critical areas like healthcare, education, and public services, where consistency and reproducibility are essential. On the other hand, our findings reveal that true reproducibility may require additional computational resources, potentially exacerbating the already significant environmental effects of LLM development. We hope our work will encouage the AI community to establity better standards of evaluation–ultimately leading to more trustworthy and reliable AI systems.

C Prompt Formats Used in Our Evaluation

Our evaluation implementation and prompt formats are adapted from SkyThought repository. AIME'24 and MATH500 share a common prompt format across all models. LiveCodeBench-Easy, LiveCodeBench-Medium, and LiveCodeBench-Hard also have the same prompt format across all models, which varies by the test type of the problems (stdin, functional). The `___PROBLEM_TEXT___` is the placeholder that will be replaced with specific problem texts from benchmarks during prompting.

C.1 MATH Benchmarks: AIME'24 and MATH500

```
DeepSeek-R1-Distill-Qwen-7B and DeepSeek-R1-Distill-Llama-8B

<|begin_of_sentence|><|User|>Return your final response within
↪ \\boxed{}.  ___PROBLEM_TEXT___<|Assistant|><think>\n
```

```
Qwen2.5-7B-Instruct

<|im_start|>system\nYou are Qwen, created by Alibaba Cloud.  You are
↪ a helpful assistant.<|im_end|>\n<|im_start|>user\nReturn your
↪ final response within \\boxed{}.  ___PROBLEM_TEXT___<|im_end|>\n
↪ <|im_start|>assistant\n
```

```
Llama-3.1-8B-Instruct

<|begin_of_text|><|start_header_id|>system<|end_header_id|>\n\nCutting
↪ Knowledge Date:  December 2023\nToday Date:  26 Jul 2024\n\n
↪ <|eot_id|><|start_header_id|>user<|end_header_id|>\n\nReturn
↪ your final response within \\boxed{}.  ___PROBLEM_TEXT___<|eot_id|>
↪ <|start_header_id|>assistant<|end_header_id|>\n\n
```

C.2 Code Generation Benchmarks: LiveCodeBench-Easy, LiveCodeBench-Medium, LiveCodeBench-Hard

---

DeepSeek-R1-Distill-Qwen-7B and DeepSeek-R1-Distill-Llama-8B

For problems with "stdin" tests:
```
<|begin_of_sentence|><|User|>Generate an executable Python function
↪ generated from the given prompt. The function should take stdin
↪ as input and print the output. Simply call the function after
↪ the definition. ___PROBLEM_TEXT___<|Assistant|><think>\n
```

For problems with "functional" tests:
```
<|begin_of_sentence|><|User|>Generate an executable Python function
↪ generated from the given prompt. Return the function body without
↪ invoking it at the final solution. ___PROBLEM_TEXT___<|Assistant|>
↪ <think>\n
```

Qwen2.5-7B-Instruct

For problems with "stdin" tests:
```
<|im_start|>system\nYou are Qwen, created by Alibaba Cloud. You are
↪ a helpful assistant.<|im_end|>\n<|im_start|>user\nGenerate an
↪ executable Python function generated from the given prompt. The
↪ function should take stdin as input and print the output. Simply
↪ call the function after the definition. ___PROBLEM_TEXT___
↪ <|im_end|>\n<|im_start|>assistant\n
```

For problems with "functional" tests:
```
<|im_start|>system\nYou are Qwen, created by Alibaba Cloud. You are
↪ a helpful assistant.<|im_end|>\n<|im_start|>user\nGenerate an
↪ executable Python function generated from the given prompt.
↪ Return the function body without invoking it at the final
↪ solution. ___PROBLEM_TEXT___<|im_end|>\n<|im_start|>assistant\n
```

Llama-3.1-8B-Instruct

For problems with "stdin" tests:
```
<|begin_of_text|><|start_header_id|>system<|end_header_id|>\n\nCutting
↪ Knowledge Date: December 2023\nToday Date: 26 Jul 2024\n\n
↪ <|eot_id|><|start_header_id|>user<|end_header_id|>\n\nGenerate an
↪ executable Python function generated from the given prompt. The
↪ function should take stdin as input and print the output. Simply
↪ call the function after the definition. ___PROBLEM_TEXT___<|eot_id|>
↪ <|start_header_id|>assistant<|end_header_id|>\n\n
```

For problems with "functional" tests:
```
<|begin_of_text|><|start_header_id|>system<|end_header_id|>\n\nCutting
↪ Knowledge Date: December 2023\nToday Date: 26 Jul 2024\n\n
↪ <|eot_id|><|start_header_id|>user<|end_header_id|>\n\nGenerate an
↪ executable Python function generated from the given prompt.
↪ Return the function body without invoking it at the final
↪ solution. ___PROBLEM_TEXT___<|eot_id|><|start_header_id|>assistant
↪ <|end_header_id|>\n\n
```
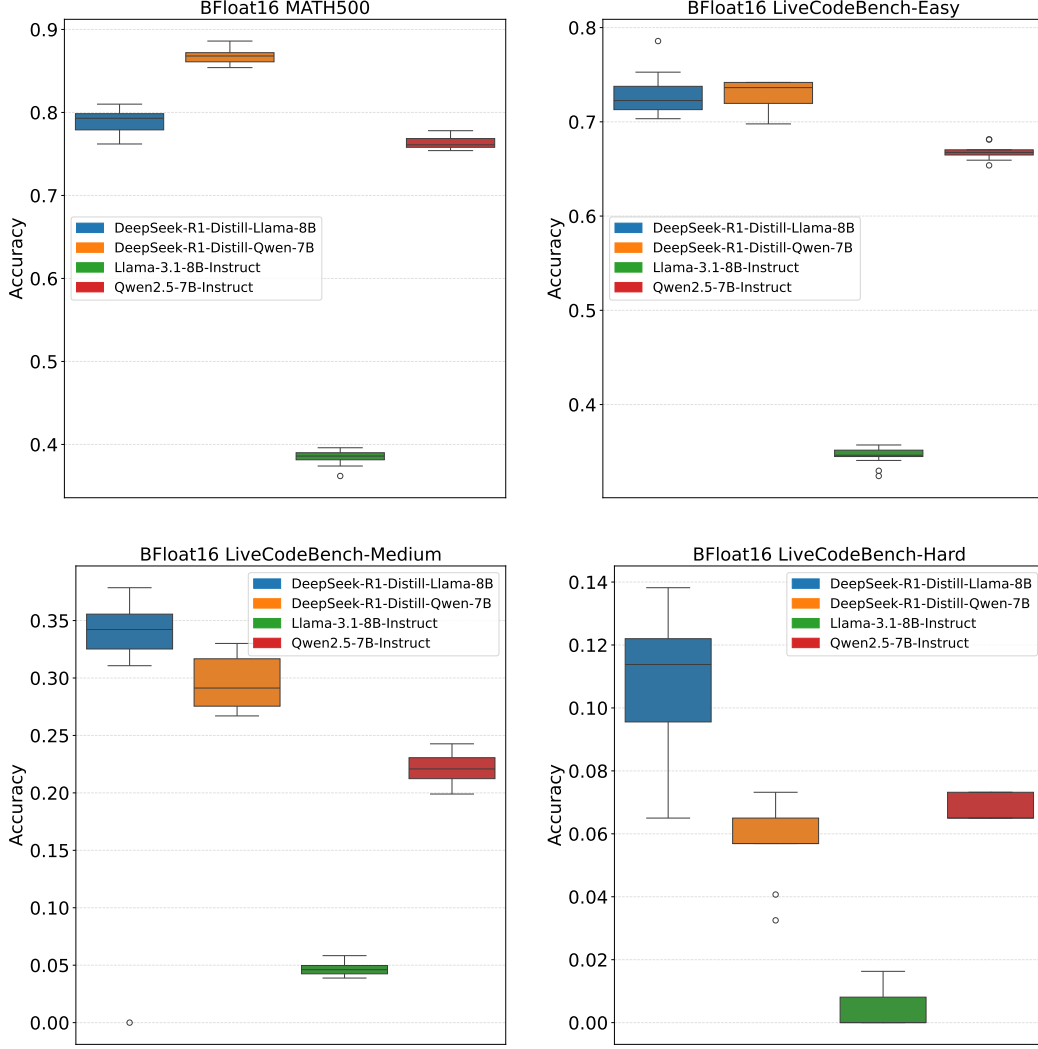
Figure 9: Accuracy varies significantly across different settings under BFloat16.

D Supplementary Results on Accuracy Variance under BFloat16

In Section 1, we demonstrated the variance of accuracy on BF16 with the same seed and greedy decoding but different batch sizes and number of GPUs in Figure 1. To provide a comprehensive understanding of reproducibility challenges across different problem domains, Figure 9 extends this analysis to all evaluated datasets. The results reveal a clear pattern: while accuracy variance under BF16 precision is relatively modest for MATH500 and LiveCodeBench-Easy, it becomes substantially more pronounced for the more challenging LiveCodeBench-Medium and LiveCodeBench-Hard benchmarks. This dataset-dependent variation suggests that the impact of numerical precision on reproducibility scales with problem complexity.

E Supplementary Results on Greedy Decoding

Following up on Figure 5 and Table 3 from Section 3.2, we present comprehensive results across all experimental settings. We report three key metrics: Std@Acc, Div_Percent, and Average Div_Index.

Table 6 presents the standard deviation of accuracy (Std@Acc) across 12 runtime configurations under BF16, FP16, and FP32 precisions for LiveCodeBench-Medium and LiveCodeBench-Hard datasets. Table 7 reports the average standard deviation of output lengths (Avg_Std@Output_Length)

Table 6: Std@Acc of greedy decoding across 12 different settings (GPU types, GPU counts, and batch sizes) under BF16, FP16, and FP32 numerical precisions on LiveCodeBench datasets

	LiveCodeBench-Medium			LiveCodeBench-Hard		
	BF16	**FP16**	**FP32**	**BF16**	**FP16**	**FP32**
DeepSeek-R1-Distill-Qwen-7B	2.28%	2.21%	0.44%	1.19%	1.98%	0.42%
DeepSeek-R1-Distill-Llama-8B	2.08%	1.84%	0.78%	2.15%	1.90%	0.53%
Qwen2.5-7B-Instruct	1.44%	0.24%	0	0.40%	1.45e-17	1.45e-17
Llama-3.1-8B-Instruct	0.70%	0.48%	0.44%	0.65%	3.62e-18	3.62e-18

Table 7: Avg_Std@Output_Length of greedy decoding across 12 different settings (GPU types, GPU counts, and batch sizes) under BF16, FP16, and FP32 numerical precisions on LiveCodeBench datasets

	LiveCodeBench-Medium			LiveCodeBench-Hard		
	BF16	**FP16**	**FP32**	**BF16**	**FP16**	**FP32**
DeepSeek-R1-Distill-Qwen-7B	8893.02	8026.63	547.50	8036.21	7476.98	646.30
DeepSeek-R1-Distill-Llama-8B	8240.77	7842.29	646.30	7518.49	6827.19	690.86
Qwen2.5-7B-Instruct	26.47	6.18	0	36.01	9.26	0
Llama-3.1-8B-Instruct	60.25	7.49	0.89	78.26	15.95	2.75

across the same 12 runtime configurations and precision settings for these two datasets. In Table 8, we measure the Div_Index of each example across 12 runtime configurations—within the 0–Div_Index range, the 12 responses corresponding to the same problem have exactly the same token at each position—and report the average Div_Index over the entire dataset. Table 9 shows the percentage of examples in each dataset exhibiting divergent outputs across the 12 runtime settings.

These results consistently support our conclusion that during greedy decoding, rounding errors from floating-point operations cause serious reproducibility problems. As numerical precision increases from BF16 to FP32, the divergence phenomenon is substantially reduced, evidenced by lower Std@Acc, lower Div_Percent, and larger Div_Index values.

F Supplementary Results on Ablation Study

Continuing the discussion from Section 3.4, we provide additional results that isolate specific runtime configurations to examine their individual effects on reproducibility. For greedy decoding experiments, we focus exclusively on BF16 and FP16 precisions, since FP32 precision effectively mitigates numerical-precision-related errors and thus provides limited insight into reproducibility challenges.

Tables 10 and 11 discuss the effect of different numbers of GPUs since, intuitively, the effect has a dependency on the GPU version, so we consider the situation on L40S and A100, separately. Table 10 reports the Avg_Std@top1_prob of LLM inference responses for the same question using 2 or 4 L40S GPUs under three different batch sizes (8, 16, and 32), while Table 11 presents the corresponding results using A100 GPUs. As shown in Table 10, increasing the number of GPUs from 2 to 4 generally leads to higher Avg_Std@top1_prob. **This observation suggests that increasing the number of GPUs may introduce greater inference nondeterminism.** However, this trend becomes less consistent in the A100 setting as shown in Table 11, where in many cases the 2 GPU results are even slightly higher than those of 4 GPUs. One reason behind it is that A100s do have higher instability in our experiments, which may have more influence beyond the number of GPUs (see Figure 6 (c)).

Table 12 examines the effect of different batch sizes. We report the Avg_Std@top1_prob of LLM inference responses for identical questions under varying GPU counts and GPU types. The results show that **larger batch sizes consistently lead to lower Avg_Std@top1_prob, indicating better**

Table 8: Average Div_Index across 12 different settings under BF16, FP16, and FP32 numerical precisions. In the table, a value of "-1" indicates that no divergence occurred for any example in the dataset under the given setting.

		DeepSeek-R1-Distill-Qwen-7B	DeepSeek-R1-Distill-Llama-8B	Qwen2.5-7B-Instruct	Llama-3.1-8B-Instruct
AIME'24	BF16	45.67	67.37	82.37	22.44
	FP16	430.13	430.47	457.41	635.43
	FP32	-1	13520	-1	1976.40
MATH500	BF16	65.33	76.85	103.58	38.07
	FP16	395.46	463.14	267.59	284.89
	FP32	1825.79	1855.17	-1	1509.61
LCB-Easy	BF16	35.11	47.43	46.98	53.99
	FP16	292.99	327.53	87.53	133.80
	FP32	1143.30	1036.04	-1	108.86
LCB-Medium	BF16	44.23	47.59	44.23	54.33
	FP16	267.81	287.83	107.07	172.73
	FP32	2291.83	2585.83	-1	125.00
LCB-Hard	BF16	43.85	31.57	43.64	54.95
	FP16	216.16	329.38	136.89	221.76
	FP32	5807.83	3832.54	-1	352.78

Table 9: Div_Percent across 12 different settings (GPU types, GPU counts, and batch sizes) under BF16, FP16, and FP32 numerical precisions

		DeepSeek-R1-Distill-Qwen-7B	DeepSeek-R1-Distill-Llama-8B	Qwen2.5-7B-Instruct	Llama-3.1-8B-Instruct
AIME'24	BF16	100%	100%	100%	53.33%
	FP16	100%	100%	73.33%	23.33%
	FP32	0	6.67%	6.67%	16.67%
MATH500	BF16	99.60%	100%	90.20%	77.60%
	FP16	86.00%	87.80%	37.60%	36%
	FP32	5.80%	6.00%	1.80%	9.20%
LCB-Easy	BF16	100%	100%	72.53%	96.15%
	FP16	100%	97.25%	16.48%	41.76%
	FP32	10.99%	13.19%	0	3.85%
LCB-Medium	BF16	100%	100%	89.32%	98.06%
	FP16	100%	100%	35.44%	48.06%
	FP32	19.90%	23.30%	0	3.40%
LCB-Hard	BF16	100%	100%	95.12%	100%
	FP16	100%	100%	50.41%	58.54%
	FP32	24.39%	30.08%	0	7.32%

reproducibility in model outputs. This finding aligns with our hypothesis that higher parallelism reduces error accumulation.

Finally, we compare the effect of the two GPU versions we used (L40S and A100). Table 13 reveals that under the same experimental settings, the Avg_Std@top1_prob on the A100 GPU is consistently slightly higher than that on the L40S GPU. **This conforms to the previous findings that, in our experiments, A100 exhibits slightly higher hardware-induced variability, which may contribute to less stable top-1 token predictions across different runtime configurations.**

Tables 14, 15, 16 and 17 present the Std@Acc for each ablation study. Unlike Avg_Std@top1_prob, it's hard to observe clear trends or patterns from Std@Acc. We argue that Avg_Std@top1_prob

Table 10: Instability (Avg_Std@top1_prob ($\times 10^{-4}$)) under different numbers of L40S GPUs

		DeepSeek-R1-Distill-Qwen-7B		DeepSeek-R1-Distill-Llama-8B		Qwen2.5-7B-Instruct		Llama-3.1-8B-Instruct	
		2GPU	4GPU	2GPU	4GPU	2GPU	4GPU	2GPU	4GPU
AIME'24	**BF16**	29.66	24.52	23.02	28.01	29.40	34.05	22.12	44.54
	FP16	5.83	5.19	3.18	3.95	2.94	3.91	2.89	7.30
MATH500	**BF16**	32.91	32.67	23.03	27.33	26.51	24.91	35.92	42.31
	FP16	4.48	4.72	3.19	3.55	3.79	3.75	4.80	5.75
LCB-Easy	**BF16**	42.80	46.82	28.46	34.80	28.48	30.31	28.05	33.93
	FP16	6.03	6.55	4.27	4.68	4.29	4.42	3.62	4.45
LCB-Medium	**BF16**	38.44	44.52	30.25	39.24	29.68	34.56	27.62	36.34
	FP16	7.04	7.68	4.52	5.00	4.84	4.74	3.45	4.05
LCB-Hard	**BF16**	38.63	48.74	29.76	36.10	34.31	29.60	28.90	34.60
	FP16	6.62	7.36	5.04	5.58	5.03	4.85	3.17	5.61

Table 11: Instability (Avg_Std@top1_prob ($\times 10^{-4}$)) under different numbers of A100 GPUs

		DeepSeek-R1-Distill-Qwen-7B		DeepSeek-R1-Distill-Llama-8B		Qwen2.5-7B-Instruct		Llama-3.1-8B-Instruct	
		2GPU	4GPU	2GPU	4GPU	2GPU	4GPU	2GPU	4GPU
AIME'24	**BF16**	32.91	33.90	31.23	25.86	30.64	41.65	53.72	35.56
	FP16	7.23	5.79	4.57	3.85	4.23	3.75	5.66	5.02
MATH500	**BF16**	34.59	30.88	31.69	25.63	26.59	21.88	43.03	44.33
	FP16	5.29	4.45	4.40	3.46	4.17	3.08	7.43	6.58
LCB-Easy	**BF16**	48.20	43.05	36.76	32.01	28.82	34.64	36.01	35.56
	FP16	7.55	6.38	6.14	4.52	4.75	4.70	5.36	4.26
LCB-Medium	**BF16**	44.86	44.26	42.58	37.60	31.02	35.01	39.96	33.40
	FP16	8.40	7.37	6.53	5.03	5.12	4.44	4.93	4.07
LCB-Hard	**BF16**	46.25	47.95	41.58	37.75	36.88	39.98	41.82	33.43
	FP16	7.95	6.79	6.63	5.41	5.11	4.76	5.29	5.88

Table 12: Instability (Avg_Std@top1_prob ($\times 10^{-4}$)) under different batch sizes

		DeepSeek-R1-Distill-Qwen-7B			DeepSeek-R1-Distill-Llama-8B			Qwen2.5-7B-Instruct			Llama-3.1-8B-Instruct		
		BS=8	BS=16	BS=32	BS=8	BS=16	BS=32	BS=8	BS=16	BS=32	BS=8	BS=16	BS=32
AIME'24	**BF16**	42.35	37.96	39.21	30.81	36.82	34.41	35.88	32.09	37.75	53.86	58.55	47.23
	FP16	6.66	6.17	6.16	4.40	4.14	4.10	4.03	4.49	3.91	3.79	4.96	3.41
MATH500	**BF16**	37.61	36.91	34.41	32.34	31.72	26.93	31.16	31.84	29.22	54.17	50.32	47.86
	FP16	5.26	5.23	4.79	4.28	4.19	3.68	3.87	3.96	3.57	6.69	5.59	6.14
LCB-Easy	**BF16**	56.00	58.99	51.39	41.93	41.56	36.80	39.14	38.27	36.21	44.63	45.88	39.60
	FP16	7.51	7.81	7.15	5.97	5.90	5.13	5.11	5.52	4.70	5.42	4.68	4.52
LCB-Medium	**BF16**	53.20	51.56	48.35	45.21	46.54	41.43	41.11	39.74	39.48	47.32	46.33	43.92
	FP16	8.55	8.36	8.11	6.21	6.25	5.46	5.98	5.94	5.95	4.92	4.68	4.52
LCB-Hard	**BF16**	57.69	59.04	54.60	47.51	47.89	41.43	49.21	47.05	46.57	46.12	44.22	39.27
	FP16	8.41	8.50	7.74	6.59	6.54	5.90	5.96	6.01	6.15	5.54	5.75	5.30

serves as a more informative metric for ablation studies, as it directly reflects the numerical instability introduced by rounding error—i.e., fluctuations in the predicted probabilities of the same token. However, such fluctuations do not always lead to a token flip, since a flip only occurs when the variation at a specific position exceeds the original top-1 and top-2 probability gap, which is inherently a stochastic event. Moreover, even when a token flip happens—for example, replacing "the" with "that"—it may not necessarily cause the evaluation outcome to change from *correct* to *incorrect* or vice versa, and thus may not affect the final accuracy.

Table 13: Instability (Avg_Std@top1_prob ($\times 10^{-4}$)) under different GPU versions

		DeepSeek-R1-Distill-Qwen-7B		DeepSeek-R1-Distill-Llama-8B		Qwen2.5-7B-Instruct		Llama-3.1-8B-Instruct	
		A100	L40S	A100	L40S	A100	L40S	A100	L40S
AIME'24	**BF16**	42.43	37.74	33.89	31.48	39.08	34.86	55.99	42.36
	FP16	7.22	6.34	4.72	4.23	4.69	4.34	6.86	6.01
MATH500	**BF16**	39.12	36.11	33.94	29.32	30.96	30.19	53.43	47.06
	FP16	5.50	5.09	4.51	3.87	4.22	4.00	6.86	5.58
LCB-Easy	**BF16**	58.36	54.88	43.33	36.87	37.45	35.12	44.84	41.29
	FP16	7.96	7.15	6.28	5.32	5.23	4.82	5.45	4.49
LCB-Medium	**BF16**	54.76	48.67	47.79	43.59	38.53	37.90	46.17	42.22
	FP16	8.81	8.26	6.67	5.65	5.54	5.59	5.08	4.62
LCB-Hard	**BF16**	60.11	54.66	49.39	42.40	47.11	44.72	45.59	40.64
	FP16	8.38	8.10	7.04	6.18	5.91	5.91	5.59	5.13

Table 14: Instability (Std@Acc) under different numbers of L40S GPUs

		DeepSeek-R1-Distill-Qwen-7B		DeepSeek-R1-Distill-Llama-8B		Qwen2.5-7B-Instruct		Llama-3.1-8B-Instruct	
		2GPU	4GPU	2GPU	4GPU	2GPU	4GPU	2GPU	4GPU
AIME'24	**BF16**	3.33%	13.47%	5.10%	1.92%	1.7e-17	1.92%	0	3.33%
	FP16	10.72%	5.10%	8.39%	1.92%	1.7e-17	1.7e-17	1.92%	1.92%
MATH500	**BF16**	1.10%	1.11%	2.53%	2.16%	0.90%	0.72%	1.70%	0.23%
	FP16	1.79%	0.64%	0.90%	0.46%	0.40%	0.46%	0.46%	0.23%
LCB-Easy	**BF16**	2.54%	1.14%	1.93%	0.64%	0.64%	0.95%	0.83%	1.27%
	FP16	1.14%	0.32%	1.10%	1.45%	0.32%	0	0.46%	0.23%
LCB-Medium	**BF16**	2.92%	3.03%	1.29%	3.12%	0.74%	1.40%	0.57%	0.84%
	FP16	3.45%	1.56%	1.71%	1.84%	0.28%	0.28%	0.84%	0.28%
LCB-Hard	**BF16**	0.94%	1.69%	2.40%	0.47%	0	0.47%	0.94%	0.47%
	FP16	2.81%	0.94%	2.15%	3.08%	0	0	0	0

Table 15: Instability (Std@Acc) under different numbers of A100 GPUs

		DeepSeek-R1-Distill-Qwen-7B		DeepSeek-R1-Distill-Llama-8B		Qwen2.5-7B-Instruct		Llama-3.1-8B-Instruct	
		2GPU	4GPU	2GPU	4GPU	2GPU	4GPU	2GPU	4GPU
AIME'24	**BF16**	5.78%	5.09%	3.85%	8.39%	1.92%	1.92%	1.92%	1.92%
	FP16	5.09%	1.92%	5.09%	6.94%	1.7e-17	1.7e-17	0	0
MATH500	**BF16**	0.61%	1.60%	0.70%	1.41%	1.29%	0.20%	0.46%	1.00%
	FP16	1.44%	0.61%	0.64%	1.11%	0.35%	0.31%	6.8e-17	0.50%
LCB-Easy	**BF16**	1.14%	2.40%	2.08%	3.22%	0.84%	0.84%	0.32%	1.14%
	FP16	2.22%	1.14%	2.48%	1.26%	0.55%	0.64%	0.64%	0.84%
LCB-Medium	**BF16**	2.39%	1.22%	1.84%	1.75%	2.12%	1.22%	0.84%	0.49%
	FP16	2.57%	2.24%	2.95%	1.28%	0	0.28%	0.49%	0.28%
LCB-Hard	**BF16**	0.94%	0.47%	1.63%	0.47%	0.47%	0.47%	0	0.47%
	FP16	1.88%	0.47%	2.05%	0.82%	0	0	0	0

Table 16: Instability (Std@Acc) under different batch sizes

		DeepSeek-R1-Distill-Qwen-7B			DeepSeek-R1-Distill-Llama-8B			Qwen2.5-7B-Instruct			Llama-3.1-8B-Instruct		
		BS=8	BS=16	BS=32	BS=8	BS=16	BS=32	BS=8	BS=16	BS=32	BS=8	BS=16	BS=32
AIME'24	BF16	7.20%	8.61%	12.58%	4.19%	5.00%	4.19%	1.92%	1.67%	0	0	2.72%	1.92%
	FP16	7.94%	5.00%	4.19%	7.39%	6.38%	3.19%	0	0	0	1.67%	1.67%	0
MATH500	BF16	0.76%	1.30%	1.12%	0.50%	2.07%	1.91%	1.00%	0.69%	0.85%	1.44%	0.44%	0.93%
	FP16	0.77%	0.82%	1.30%	0.35%	0.97%	0.50%	0.43%	0.35%	0.33%	0.35%	0.35%	0.16%
LCB-Easy	BF16	1.80%	2.12%	0.78%	1.82%	1.45%	3.11%	0.45%	1.30%	0.32%	1.22%	0.52%	1.29%
	FP16	1.38%	1.34%	1.00%	1.45%	2.70%	0.95%	0.69%	0.28%	0.53%	0.94%	0.64%	0
LCB-Medium	BF16	1.95%	2.79%	2.38%	1.90%	0.89%	3.13%	1.65%	0.83%	0.89%	0.80%	0.73%	0.46%
	FP16	2.22%	3.23%	0.25%	2.64%	0.79%	0.69%	0.28%	0.24%	0.24%	0.63%	0.40%	0.46%
LCB-Hard	BF16	0.67%	1.68%	1.02%	2.05%	1.68%	3.15%	0.47%	0.41%	0.41%	0.78%	0	0.78%
	FP16	2.24%	2.39%	1.67%	2.53%	2.14%	1.41%	0	0	0	0	0	0

Table 17: Instability (Std@Acc) under different GPU versions

		DeepSeek-R1-Distill-Qwen-7B		DeepSeek-R1-Distill-Llama-8B		Qwen2.5-7B-Instruct		Llama-3.1-8B-Instruct	
		A100	L40S	A100	L40S	A100	L40S	A100	L40S
AIME'24	BF16	5.44%	11.81%	5.87%	3.44%	1.82%	1.72%	1.72%	2.11%
	FP16	3.50%	7.72%	5.96%	6.55%	1.52e-17	1.52e-17	0	1.72%
MATH500	BF16	1.14%	1.01%	1.03%	2.11%	0.84%	0.83%	0.72%	1.17%
	FP16	0.99%	1.21%	0.83%	0.64%	0.33%	0.39%	0.35%	0.34%
LCB-Easy	BF16	1.69%	1.79%	2.66%	1.42%	0.90%	0.75%	9.59%	1.08%
	FP16	1.58%	0.96%	1.76%	2.14%	0.67%	0.22%	0.73%	0.45%
LCB-Medium	BF16	1.76%	2.70%	2.20%	2.16%	1.83%	1.04%	0.62%	0.67%
	FP16	2.16%	2.41%	2.19%	1.62%	0.35%	0.25%	0.40%	0.57%
LCB-Hard	BF16	6.65%	1.51%	2.61%	1.58%	0.45%	0.33%	0.33%	0.80%
	FP16	1.82%	2.14%	1.52%	2.38%	0	0	0	0

G   Supplementary Results on LayerCast

We evaluate the LayerCast method proposed in Section 4 using the DeepSeek-R1-Distill-Qwen-7B model across five benchmarks: AIME'24, MATH500, LiveCodeBench-Easy, LiveCodeBench-Medium, and LiveCodeBench-Hard. These evaluations span different batch sizes (8, 16, 32), GPU counts (2 and 4), and numerical precision settings (BF16, FP32, and LayerCast). All LayerCast experiments follow the same experimental configuration as our main studies.

Table 18 reports both the accuracy and its standard deviation across different GPU count and batch size configurations. To facilitate comparison, results under FP32 and BF16 are also included. As expected, BF16 exhibits the most instability, with significantly higher standard deviations. LayerCast matches FP32 in terms of stability (often with zero or near-zero std) while preserving memory efficiency. These results corroborate our main findings in Section 4, demonstrating that LayerCast delivers reproducibility on par with FP32 while operating within a lower memory footprint.

H   Supplementary Results on Random Sampling

In this section, we show more results related to the discussion in Section 3.3. In the random sampling setting, we report the complete set of Pass@1 results in AIME'24 and MATH500 to further evaluate reproducibility under different precision settings. These experiments are conducted across different batch sizes (8, 16, 32), and GPU counts (2 and 4). The standard deviations are calculated along numeric precision types (BF16, FP16, FP32).

Tables 19, 21, 20, and 22 summarize the Pass@1 accuracies and their standard deviation on DeepSeek-R1-Distill-Qwen-7B, DeepSeek-R1-Distill-Llama-8B, Qwen2.5-7B-Instruct, Llama-3.1-8B-Instruct, respectively. In most cases, FP32 yields the lowest standard deviations, reflecting greater stability across configurations. However, it is worth noticing that there are (4 out of 12) cases where FP16

results are more stable. This suggests that during random sampling, the two sources of randomness can interleave. We still urge researchers to sample more extensively to obtain more reproducible results.

Table 18: Accuracy and standard deviation of DeepSeek-R1-Distill-Qwen-7B under different GPU counts, precisions (including LayerCast), and batch sizes across 5 benchmarks.

Benchmark	2x A100			4x A100			Std@Acc
	BS=8	BS=16	BS=32	BS=8	BS=16	BS=32	
AIME'24							
LayerCast	0.4333	0.4333	0.4333	0.4333	0.4333	0.4333	**0**
FP32	0.4333	0.4333	0.4333	0.4333	0.4333	0.4333	**0**
BF16	0.4667	0.4667	0.3667	0.4333	0.5333	0.4667	**0.0544**
MATH500							
LayerCast	0.8680	0.8680	0.8680	0.8660	0.8660	0.8660	**0.0011**
FP32	0.8680	0.8680	0.8680	0.8680	0.8660	0.8700	**0.0013**
BF16	0.8700	0.8620	0.8580	0.8540	0.8860	0.8700	**0.0114**
LCB-Easy							
LayerCast	0.7308	0.7308	0.7363	0.7363	0.7418	0.7418	**0.0049**
FP32	0.7363	0.7363	0.7363	0.7308	0.7363	0.7363	**0.0022**
BF16	0.7198	0.7418	0.7253	0.7418	0.6978	0.7363	**0.0169**
LCB-Medium							
LayerCast	0.3058	0.3010	0.2961	0.2961	0.3010	0.3058	**0.0043**
FP32	0.3058	0.3010	0.3058	0.3058	0.3058	0.3010	**0.0025**
BF16	0.2816	0.2767	0.3204	0.2961	0.2864	0.2718	**0.0176**
LCB-Hard							
LayerCast	0.0488	0.0488	0.0569	0.0569	0.0488	0.0569	**0.0044**
FP32	0.0488	0.0488	0.0488	0.0569	0.0569	0.0569	**0.0044**
BF16	0.0569	0.0732	0.0569	0.0650	0.0569	0.0650	**0.0066**

Table 19: Pass@1 accuracies (%) under 6 system configurations and the standard deviation across them for DeepSeek-R1-Distill-Qwen-7B.

	2x A100			4x A100			Stdev
	BS=8	BS=16	BS=32	BS=8	BS=16	BS=32	
AIME'24, n=16							
FP32	53.33	56.25	55.21	53.13	54.17	54.17	**1.1784**
FP16	52.71	55.00	52.92	53.33	53.13	53.13	**0.8273**
BF16	53.33	56.88	55.42	56.67	53.54	53.13	**1.7151**
AIME'24, n=64							
FP32	54.38	54.12	53.39	54.74	54.38	55.63	**0.7377**
FP16	54.27	54.06	55.52	54.38	54.11	54.38	**0.5391**
BF16	54.74	54.17	55.10	54.90	55.16	55.10	**0.3749**
MATH500, n=4							
FP32	90.60	90.80	90.80	90.75	90.90	90.70	**0.1021**
FP16	90.25	90.20	90.20	90.45	90.50	90.15	**0.1463**
BF16	90.65	91.15	90.40	90.95	90.85	90.35	**0.3158**

Table 20: Pass@1 accuracies (%) under 6 system configurations and the standard deviation across them for DeepSeek-R1-Distill-Llama-8B.

	2x A100			4x A100			Stdev
	BS=8	BS=16	BS=32	BS=8	BS=16	BS=32	
AIME'24, n=16							
FP32	43.33	43.75	41.88	42.92	43.96	42.08	**0.8606**
FP16	43.96	45.63	43.75	41.04	40.83	42.08	**1.8792**
BF16	46.46	45.42	42.71	43.13	43.54	43.13	**1.5124**
AIME'24, n=64							
FP32	43.65	43.39	44.22	44.48	43.33	44.32	**0.5034**
FP16	43.49	44.22	44.17	42.87	42.60	42.14	**0.8539**
BF16	43.13	42.76	43.07	41.41	41.98	43.85	**0.8774**
MATH500, n=4							
FP32	83.85	83.95	83.75	83.65	83.95	83.75	**0.1211**
FP16	84.55	83.95	83.95	84.15	84.25	83.55	**0.3371**
BF16	84.50	84.80	84.35	84.60	85.20	85.20	**0.3602**

Table 21: Pass@1 accuracies (%) under 6 system configurations and the standard deviation across them for Qwen2.5-7B-Instruct.

	2x A100			4x A100			Stdev
	BS=8	BS=16	BS=32	BS=8	BS=16	BS=32	
AIME'24, n=16							
FP32	11.46	11.46	11.46	11.46	11.46	11.46	**0**
FP16	11.04	11.67	11.46	11.25	11.67	11.25	**0.2523**
BF16	11.25	10.21	11.04	9.38	11.04	10.42	**0.7056**
AIME'24, n=64							
FP32	11.25	11.25	11.25	11.25	11.25	11.25	**0**
FP16	10.99	11.25	11.25	11.20	11.41	11.30	**0.1382**
BF16	11.20	11.04	11.41	11.04	11.30	10.94	**0.1784**
MATH500, n=4							
FP32	74.85	74.85	74.85	74.80	74.80	74.80	**0.0274**
FP16	74.50	74.90	74.80	75.00	74.80	74.75	**0.1686**
BF16	90.65	91.15	90.40	90.95	90.85	90.35	**0.3158**

Table 22: Pass@1 accuracies (%) under 6 system configurations and the standard deviation across them for Llama-3.1-8B-Instruct.

	2x A100			4x A100			Stdev
	BS=8	BS=16	BS=32	BS=8	BS=16	BS=32	
AIME'24, n=16							
FP32	5.00	5.42	3.75	5.00	5.42	3.75	**0.7759**
FP16	5.00	5.00	4.58	5.21	5.00	5.21	**0.2282**
BF16	3.96	4.38	4.79	5.42	5.21	5.42	**0.5992**
AIME'24, n=64							
FP32	4.01	4.01	4.27	4.01	4.06	4.27	**0.1296**
FP16	3.91	4.06	4.17	4.22	4.58	4.64	**0.2898**
BF16	4.01	3.70	4.32	4.01	4.90	3.91	**0.4216**
MATH500, n=4							
FP32	37.00	36.50	36.30	36.80	36.30	36.15	**0.3293**
FP16	37.10	36.60	37.00	36.90	36.95	37.00	**0.1725**
BF16	36.25	36.95	36.65	35.35	35.90	36.75	**0.6020**